Title

A circulating tumor cell-based digital assay for the detection of EGFR T790M mutation in advanced non-small cell lung cancer

Journal

Journal of Materials Chemistry B, 8(26)

ISSN

2050-750X

Authors

Wang, Jing
Sun, Na
Lee, Yi-Te
et al.

Publication Date

2020-07-08

DOI

10.1039/d0tb00589d

Peer reviewed

HHS Public Access

Author manuscript

J Mater Chem B. Author manuscript; available in PMC 2021 May 20.

Published in final edited form as:

J Mater Chem B. 2020 July 08; 8(26): 5636–5644. doi:10.1039/d0tb00589d.

A circulating tumor cell-based digital assay for the detection of EGFR T790M mutation in advanced non-small cell lung cancer†

Jing Wang[a,b], **Na Sun**[b,c], **Yi-Te Lee**[b], **Yiqian Ni**[d], **Rose Koochekpour**[b], **Yazhen Zhu**[b], **Hsian-Rong Tseng**[b], **Shuyang Wang**[a], **Liyan Jiang**[d], **Hongguang Zhu**[a]

[a]Department of Pathology, School of Basic Medical Sciences, Fudan University, Shanghai, 200032, P. R. China

[b]California NanoSystems Institute, Crump Institute for Molecular Imaging, Department of Molecular and Medical Pharmacology, University of California, Los Angeles, CA 90095, USA

[c]Key Laboratory for Nano-Bio Interface, Suzhou Institute of Nano-Tech and Nano-Bionics, University of Chinese Academy of Sciences, Chinese Academy of Sciences, Suzhou 215123, P. R. China

[d]Department of Respiratory Medicine, Shanghai Chest Hospital, Shanghai Jiao Tong University, Shanghai, 200030, P. R. China

Abstract

Determining the status of epidermal growth factor receptor (EGFR) T790M mutation is crucial for guiding further treatment intervention in advanced non-small cell lung cancer (NSCLC) patients who develop acquired resistance to initial EGFR tyrosine kinase inhibitor (TKI) treatment. Circulating tumor cells (CTCs) which contain plentiful copies of well-preserved RNA offer an ideal source for noninvasive detection of T790M mutation in NSCLC. We developed a CTC-based digital assay which synergistically integrates NanoVelcro Chips for enriching NSCLC CTCs and reverse-transcription droplet digital PCR (RT-ddPCR) for quantifying T790M transcripts in the enriched CTCs. We collected 46 peripheral arterial and venous blood samples from 27 advanced NSCLC patients for testing this CTC-based digital assay. The results showed that the T790M mutational status observed by the CTC-based digital assay matched with those observed by tissue-based diagnostic methods. Furthermore, higher copy numbers of T790M transcripts were observed in peripheral arterial blood than those detected in the matched peripheral venous blood. In short, our results demonstrated the potential of the NanoVelcro CTC-digital assay for noninvasive detection of the T790M mutation in NSCLC, and suggested that peripheral arterial blood sampling may offer a more abundant CTC source than peripheral venous blood in advanced NSCLC patients.

†Electronic supplementary information (ESI) available: Other supporting data.
See DOI: 10.1039/d0tb00589d

hongguang_702@163.com; Tel: +86-021-54237528-2323.

Conflicts of interest

There are no conflicts to declare.

Introduction

Lung cancer is the leading cause of cancer-related death worldwide,[1] of which non-small cell lung cancer (NSCLC) accounts for approximately 70–80%.[2] Up to 40–48% of Asian NSCLC patients are associated with activating oncogenic driver mutations in their epidermal growth factor receptor (EGFR) genes.[3] First- and second-generation EGFR tyrosine kinase inhibitors (EGFR TKIs, *e.g.*, gefitinib, erlotinib, and dacomitinib) exhibit good responses in NSCLC patients with the EGFR mutation compared with standard chemotherapy.[4,5] However, almost all patients who initially respond to an EGFR TKI subsequently develop disease progression. Many studies have been reported on the mechanisms of drug resistance to EGFR-TKIs.[6] A secondary substitution of methionine for threonine at position 790 (T790M) mutation in EGFR exon 20 is regarded as the most common resistance mechanism seen in 50–60% of patients. Osimertinib, a third generation EGFR TKI, has been approved by the Food and Drug Administration (FDA) for the treatment of progressive NSCLC patients with T790M mutation.[7,8] Therefore, detecting the T790M mutation is critical in guiding the treatment of NSCLC patients receiving EGFR TKIs. Currently, an additional biopsy is required for detecting the T790M mutation. This invasive procedure, however, may not be feasible in patients with preexisting poor health. Additionally, a single biopsy may be unable to encompass the temporal and spatial heterogeneity of the tumor.[9,10] Thus, there is an unmet need for developing a noninvasive diagnostic solution to assess and monitor the T790M mutation status throughout the EGFR TKI treatment.[11–15]

The FDA has approved the first liquid biopsy companion diagnostic with the COBAS®EGFR Mutation Test version 2, which evaluates the T790M mutation status using cell-free DNA (cfDNA). However, due to the high fragmentation of cfDNA, which is compounded by substantial background,[16] its performance for the T790M detection is limited, with a sensitivity and specificity of 58% and 80%, respectively.[17] In addition, cfDNA originates from cells undergoing apoptosis or necrosis, which may not reflect the viable cell population of the tumor.[18] Alternatively, circulating tumor cells (CTCs) are actively shed from living tumors, allowing them to be considered a surrogate tumor source.[19] Also, the intact genomic DNA and RNA are protected by cell membranes, providing biological fidelity about the tumors and offering a potentially noninvasive approach for understanding the underlying tumor biology. Over the past decades, there have been a wide spectrum of CTC detection technologies,[20,21] including (i) immunomagnetic separation for positively selecting CTCs[22,23] by targeting CTC surface markers (*e.g.*, CellSearch Assay), or negatively depleting[24] white blood cells (WBCs); (ii) flow cytometry, which utilizes fluorescent immunoaffinity agents[25] to analyze or sort CTCs; (iii) microfluidic devices that operate by the principles of immunoaffinity enrichment,[26,27] size-based sorting,[28] or an integrated approach;[29] and (iv) microscopy imaging,[30] along with other existing methodologies. Recently, researchers have shifted focus away from the capture and enumeration of CTCs, and instead, towards utilizing CTCs for the identification of therapeutic targets, stratification of patients for targeted therapies, and uncovering resistance mechanisms.[31–37] CTC-based assays have been developed for the detection of the T790M mutation utilizing CTC-derived DNA.[38] Since cancer cells actively synthesize proteins for

proliferation, CTCs often have increased levels of mRNA.[39] As such, using CTC mRNA may improve the sensitivity of T790M detection.

Here, we leveraged our previous studies[40–44] to develop a novel NanoVelcro CTC-digital assay by coupling (i) NanoVelcro Chips (Fig. S1, ESI†) for CTC enumeration, in which capture agent-coated nanosubstrates are used to selectively enrich CTCs and (ii) reverse-transcription droplet digital PCR (RT-ddPCR) for the quantification of T790M transcripts in the enriched CTCs. Pulmonary venous CTCs have been proven to be better predictors of early-stage NSCLC recurrence after surgery than peripheral CTCs due to the proximity to the primary tumor and the blood draw upstream of capillary bed filtering.[45,46] Inspired by this concept, we collected paired peripheral arterial and venous blood samples from advanced NSCLC patients and processed these samples using the workflow in Fig. 1. The resulting CTC-derived T790M transcript readouts in 12 of 12 (100%) samples from 7 T790M-positive patients were identified as positive, and 34 of 34 (100%) samples from 20 T790M-negative patients were identified as negative. Furthermore, it is worth mentioning that higher copy numbers of T790M transcripts were observed in peripheral arterial CTCs than in matched peripheral venous CTCs in T790M-positive patients. Our results demonstrated the great prospects of the NanoVelcro CTC-digital assay for detecting T790M mutation in a noninvasive fashion, and indicated that peripheral arterial blood sampling may offer a more abundant CTC source than peripheral venous blood in advanced NSCLC patients.

Experimental materials and methods

Materials for validation studies

The NCI-H1975 cell line (harboring T790M mutation), obtained from the American Type Culture Collection (ATCC), was selected to test the performance of the NanoVelcro CTC-digital assay for T790M detection. Peripheral venous blood samples from healthy donors (HDs) were obtained with the appropriate oversight from the Shanghai Chest Hospital. Peripheral blood mononuclear cells (PBMCs) from the blood of HDs were then obtained using the blood sample processing method described below. The artificial blood samples were prepared by spiking different amounts of H1975 cells into 2×10^6 PBMCs from 2 mL of healthy donor's blood in an RPMI medium (Corning, VA, USA). We conducted the NanoVelcro CTC-digital assay according to the methods described below. Each of the healthy donors' and artificial blood samples was tested in triplicate.

Patients and sample selection

Peripheral arterial and/or venous blood samples for this study were collected from the Shanghai Chest Hospital and informed consent was obtained from all participants. This study was conducted in accordance with the Declaration of Helsinki and Good Clinical Practice guidelines. Patients with histologically confirmed, advanced NSCLC who underwent evaluation and/or EGFR TKI treatment at the Shanghai chest hospital between

†Electronic supplementary information (ESI) available: Other supporting data.
See DOI: 10.1039/d0tb00589d

September 2017 and September 2018 were enrolled. These patients were further classified into the T790M-positive group or the T790M-negative group, based on their EGFR mutation statuses as confirmed by test results of tissue biopsies or cfDNA. All treatments and radiographic examinations were performed as part of ongoing clinical care. Both pre-treatment and on-treatment blood samples were analyzed when possible.

Blood sample processing

Peripheral arterial and/or venous blood was collected from radial arteries and median cubital veins, respectively, in acid-citrate dextrose-containing vacutainers (BD Bioscience, CA, USA). All the blood samples were processed within 4 hours upon collection and centrifuged at 300*g* for 5 min and then at 2000*g* for 5 min at 4 °C. Plasma was collected and stored at −80 °C. PBMCs, including CTCs, were separated by gradient centrifugation at room temperature with the use of Ficoll-Paque solution (Sigma-Aldrich, MO, USA) following the manufacturer's protocol. After washing with PBS, the PBMCs were re-suspended in 200 μL PBS for enrichment by the NanoVelcro Chips.

NanoVelcro Chips

The NanoVelcro Chip is composed of an overlaid PDMS-based chaotic mixer, a patterned silicon nanowire (SiNW) substrate, and a multilayer chip holder to assemble both functional components together.[41] The chip holder compresses the PDMS-based chaotic mixer against the channels of the silicon nanowire chip to create a microfluidic channel which optimizes cellular interactions with the chip surface. In the cutout, the nanowire substrate can be seen functionalized with streptavidin, which is used for the enrichment of biotinylated capture antibody (*i.e.*, anti-EpCAM) labeled CTCs. The detailed manufacturing materials and methods of the NanoVelcro Chips can be found in the ESI† Methods and Fig. S1.

Immunofluorescence characterization of CTCs captured from blood samples

A three-color immunocytochemistry analysis was adopted for immunofluorescence characterization of CTCs and background WBCs captured on the NanoVelcro Chips from artificial blood samples.[47] In brief, the captured CTCs were incubated with 0.05% Triton X-100 [in PBS (200 μL)] for 10 min. The captured cells were incubated overnight with a mixture of primary antibodies, including the Pan-CK antibody [rabbit, polyclonal, 1 : 100 (v/v); Dako] and anti-CD45 antibody [F10–89-4] [mouse, monoclonal, 1 : 400 (v/v); Abcam], in a PBS solution (200 μL) containing 2% normal donkey serum (Jackson ImmunoResearch) at 4 °C. After washing with PBS three times, the captured cells were further incubated at room temperature for 1 hour with a mixture of secondary antibodies, including donkey anti-rabbit IgG (H + L) [Alexa Fluor 488, 1 : 500 (v/v); Invitrogen] and donkey anti-mouse IgG (H + L) [Alexa Fluor 647, 1 : 500 (v/v); Invitrogen], in a PBS solution (200 μL) containing 2% donkey serum. After washing with PBS three times, the cells were treated with ProLong Gold Antifade Mountant with DAPI (Invitrogen). The substrates were then imaged with a fluorescence microscope (Nikon 90i). The captured CTCs were differentiated from background WBCs according to their unique staining pattern (CK+/CD45−/DAPI+) and intact nuclear morphology (WBCs were stained CK−/CD45+/DAPI+).

RNA extraction and RT-ddPCR

After being enriched by the NanoVelcro Chips, the captured fresh cells were lysed directly on the chips, and the RNA was extracted using the Direct-zol– RNA MicroPrep (Zymo Research, CA, USA) kit following the manufacturer's protocol. The cells were then lysed with 600 μL of Trizol solution and mixed with 600 μL of ethanol. The mixed solution was put into the Zymo-Spin™ IIC Column and centrifuged. After centrifugation, the solution was washed twice with the supplied wash buffer. The RNA was eluted from the column using 10 μL of RNA grade water. The amount of the eluted RNA needed was above 2 ng μL $^{-1}$ to pass the internal quality control. 3.8 μL RNA was then subjected to reverse transcription to convert it to 6 μL cDNA using the Prime-Script® RT reagent Kit (Takara, RR037A) following the manufacturer's instructions, and 2 μL cDNA was detected using the PrimePCR ddPCR Mutation Assay Kit (dHsaCP2000020, EGFR T790M mutation, Bio-Rad, USA) following the manufacturer's protocol. For the ddPCR of each sample, droplets were generated within a DG8 Cartridge which was preloaded with the sample (20 μL) and the droplet generation oil (70 μL). All droplets were then transferred into a 96-well plate, accordingly, and sealed with a PX1 PCR Plate Sealer. A programmed Thermal Cycler was set at 96 ° C for 10 min, followed by 40 cycles of 94 °C for 30 s and 60 °C for 60 s, and finally 98 °C for 10 min. The droplets containing amplicons were quantified with a QX200 Droplet Reader using the QuantaSoft software package.

Statistical analysis

We performed linear regression analysis to assess the linearity of the copy numbers of T790M transcripts and T790M genomic DNA copy numbers in H1975 cells. The slopes and coefficients of determination (*R*-squared) were calculated. For the 46 blood samples from 27 patients, a *t*-test was used to assess the differences in the copy numbers of T790M transcripts between T790M-positive patients and T790M-negative patients. A paired *t*-test was performed to check the differences in T790M transcripts between peripheral arterial and venous blood samples. The statistical tests in this study were performed using Graph-Pad Prism 7 (https://www.graphpad.com/). All tests are two-sided and $P < 0.05$ is considered statistically significant.

Results and discussion

Technical optimization and validation of the NanoVelcro CTC-digital assay

To test the sensitivity and dynamic range of the NanoVelcro CTC-digital assay for the quantification of T790M transcripts, we firstly optimize and validate the NanoVelcro Chips for CTC enrichment. We prepared artificial blood samples spiked with 200 H1975 cells (harboring T790M mutation) and processed the samples using the workflow in Fig. 2A. The influence of the flow rate on the capture efficiency of NanoVelcro Chips was firstly studied. In detail, 2 mL artificial blood samples were injected into NanoVelcro Chips at flow rates of 0.2, 0.5, 1.0, and 2.0 mL h^{-1}. An optimal capture efficiency of 86.8 ± 3.6% was obtained at a flow rate of 0.5 mL h^{-1} (Fig. S2, ESI†). Then, we performed H1975 cell capture tests with different biotinylated anti-EpCAM concentrations (*i.e.*, 0.01, 0.1, 1.0, and 2.0 μg mL^{-1}) at the optimal flow rate. Up to 85.3 ± 5% capture efficiency could be observed with an antibody concentration of 1.0 μg mL^{-1}. When the concentration was higher than 1.0 μg mL

$^{-1}$, the CTC-capture efficiency was not improved visibly (Fig. 2B). Using the optimal CTC-capture conditions, we compared the capture efficiency of NanoVelcro Chips with the commonly used CTC enrichment method, immunomagnetic beads. The immunomagnetic bead-based sorting method exhibited a capture efficiency of 46 ± 2% (Fig. 2C). These results demonstrate the superiority of NanoVelcro Chips for CTC enrichment.

We then tested the capture efficiency of the NanoVelcro Chips for enriching different numbers of CTCs using artificial blood samples. Artificial blood samples were prepared by spiking different numbers of H1975 cells (n = 5, 10, 50, 100 and 200 cells) into PBMCs from 2 mL of healthy donor's blood to mimic clinical blood samples.[40–42] The results are summarized in Fig. 2D, and showed that the capture efficiency (average 86.8%) remained consistent over the range of spiked H1975 cell numbers. Fig. 2E shows the representative fluorescence micrographs of CTCs and WBCs captured from artificial blood samples. Although there were consistent background WBCs trapped on the NanoVelcro Chips from healthy donors' blood control (4738 ± 420, in triplicate) and the artificial blood samples (4679 ± 392, in triplicate), NanoVelcro Chips achieved the ratio of CTCs to WBCs ranging from 0.1% to 3% using artificial blood samples spiked with different numbers of H1975 cells (n = 5, 10, 50, 100 and 200 cells) into PBMCs from 2 mL of healthy donor's blood, which is feasible for downstream molecular analysis.[48]

After optimizing and validating the capture efficiency of the NanoVelcro Chips for the enrichment of NSCLC CTCs, we processed the samples using the workflow described in Fig. 3A to test the feasibility of using the NanoVelcro CTC-digital assay for the quantification of T790M transcripts. We firstly quantified the T790M transcripts in different amounts of H1975 cells. A good linear correlation was observed between the copy numbers of T790M transcripts and the H1975 cell numbers (R^2 = 0.998, Fig. 3B). In the artificial blood samples processed through the NanoVelcro CTC-digital assay using H1975 cells, the resulting T790M transcript readouts also greatly correlated with the spiked H1975 cell numbers (R^2 = 0.997, Fig. 3C). Using the correlation between the copy numbers of T790M transcripts in the captured H1975 cells and the copy numbers of the T790M transcripts in H1975 cells, up to 81% capture efficiency could be achieved, which is consistent with our enumeration study above (Fig. 2).Subsequently, we explored the linear correlation between the copy numbers of T790M transcripts and T790M genomic DNA copy numbers in the captured H1975 cells using different amounts of H1975 cells through the NanoVelcro CTC-digital assay. The results showed that the copy numbers of T790M transcripts were 41.6 ± 5.7 times of the T790M genomic DNA copy numbers, demonstrating a broader dynamic range of the T790M transcripts than the T790M genomic DNA copy numbers for T790M mutation detection (Fig. 3D).

Altogether, the NanoVelcro CTC-digital assay demonstrates a high capacity for the quantification of T790M transcripts in artificial blood samples of NSCLC cells with background WBCs, paving the way for further testing in clinical blood samples.

NanoVelcro CTC-digital assay results in patient samples

We collected a total of 46 peripheral arterial/venous blood samples from 27 advanced NSCLC patients at different time points over the course of EGFR TKI treatment. Detailed

information of NSCLC patients and HDs are shown in Table 1 and Table S1 (ESI†), respectively. We performed CTC enrichment and quantification of T790M transcripts using the NanoVelcro CTC-digital assay. After normalization, the copy numbers of T790M transcripts in the CTCs captured from 2 mL peripheral arterial/venous blood samples of NSCLC patients are shown in Table 1. We compared the differences in the copy numbers of T790M transcripts enriched from both peripheral arterial/venous blood samples in NSCLC CTCs between T790M-positive patients ($n = 12$) and T790M-negative patients ($n = 34$). The copy numbers of T790M transcripts were higher in peripheral arterial/venous blood samples from T790M-positive patients compared to T790M-negative patients (t-test, $P < 0.0001$*, Fig. 4A). Next, we compared the copy numbers of T790M transcripts between paired peripheral arterial and venous CTCs ($n = 5$) from T790M-positive NSCLC patients (Fig. 4B). The copy numbers of T790M transcripts were higher in peripheral arterial CTCs when compared with the copy numbers of T790M transcripts in matched peripheral venous CTCs with statistical significance (pairwise t-test, $P = 0.03$), while there was no detectable difference in the copy numbers of T790M transcripts between paired peripheral arterial CTCs and venous CTCs ($n = 14$) from T790M-negative patients ($P > 0.05$, Fig. 4C). In this study, we compared the copy numbers of T790M transcripts from peripheral arterial CTCs with the copy numbers of T790M transcripts from paired peripheral venous CTCs. Although higher copy numbers of T790M transcripts were observed in peripheral arterial CTCs of T790M-positive patients, the resulting T790M transcript readouts in peripheral arterial CTCs from T790M-negative patients still were identified as negative, further showing the high specificity of the NanoVelcro CTC-digital assay.

Overall, the NanoVelcro CTC-digital assay has demonstrated 100% sensitivity and specificity for the detection of the T790M mutation in our study. In addition, peripheral arterial blood sampling may offer a more abundant CTC source than peripheral venous blood in advanced NSCLC patients.

Conclusions

In this study, we successfully developed and validated the NanoVelcro CTC-digital assay by coupling NanoVelcro Chips, for highly efficient enrichment of NSCLC CTCs, with a sensitive downstream RT-ddPCR, for the quantification of T790M transcripts. We demonstrated the feasibility of transforming clinically relevant tissue-based molecular phenotyping such as EGFR mutation into CTC-based tests. Although a larger, independent cohort is needed to confirm its clinical utility, the resulting CTC-derived T790M transcript readouts from both peripheral arterial and venous blood samples exhibited great capacity for detecting the EGFR T790M mutation in a noninvasive fashion, and indicated that the peripheral arterial blood sampling may offer an alternative CTC source complementary to peripheral venous blood in advanced NSCLC patients, highlighting the potential of the NanoVelcro CTC-digital assay for serially monitoring the T790M mutation status to optimize clinical treatments of advanced NSCLC patients with underlying EGFR mutations.

Supplementary Material

Refer to Web version on PubMed Central for supplementary material.

Acknowledgements

We acknowledge all the patients and healthy donors who participated in this study. Dr J. Wang gratefully acknowledges financial support from the Department of Pathology, School of Basic Medical Sciences, Fudan University.

References

1. Bray F, Ferlay J, Soerjomataram I, Siegel RL, Torre LA and Jemal A, Ca-Cancer J. Clin, 2018, 68, 394–424. [PubMed: 30207593]
2. Chen Z, Fillmore CM, Hammerman PS, Kim CF and Wong K-K, Nat. Rev. Cancer, 2014, 14, 535–546. [PubMed: 25056707]
3. Shi Y, Au JS-K, Thongprasert S, Srinivasan S, Tsai C-M, Khoa MT, Heeroma K, Itoh Y, Cornelio G. and Yang P-C, J. Thorac. Oncol, 2014, 9, 154–162. [PubMed: 24419411]
4. Pao W. and Chmielecki J, Nat. Rev. Cancer, 2010, 10, 760–774. [PubMed: 20966921]
5. Balak MN, Gong Y, Riely GJ, Somwar R, Li AR, Zakowski MF, Chiang A, Yang G, Ouerfelli O, Kris MG, Ladanyi M, Miller VA and Pao W, Clin. Cancer Res, 2006, 12, 6494–6501. [PubMed: 17085664]
6. Shea M, Costa DB and Rangachari D, Ther. Adv. Respir. Dis, 2016, 10, 113–129. [PubMed: 26620497]
7. Kobayashi S, Boggon TJ, Dayaram T, Jänne PA, Kocher O, Meyerson M, Johnson BE, Eck MJ, Tenen DG and Halmos B, N. Engl. J. Med, 2005, 352, 786–792. [PubMed: 15728811]
8. Mok TS, Wu Y-L, Ahn M-J, Garassino MC, Kim HR, Ramalingam SS, Shepherd FA, He Y, Akamatsu H, Theelen WSME, Lee CK, Sebastian M, Templeton A, Mann H, Marotti M, Ghiorghiu S. and Papadimitrakopoulou VA, N. Engl. J. Med, 2017, 376, 629–640. [PubMed: 27959700]
9. Mao C, Yuan J-Q, Yang Z-Y, Fu X-H, Wu X-Y and Tang J-L, Medicine, 2015, 94, e775. [PubMed: 26020382]
10. Lokhandwala T, Bittoni MA, Dann RA, D'Souza AO, Johnson M, Nagy RJ, Lanman RB, Merritt RE and Carbone DP, Clin. Lung Cancer, 2017, 18, e27–e34. [PubMed: 27530054]
11. Karlovich C, Goldman JW, Sun J-M, Mann E, Sequist LV, Konopa K, Wen W, Angenendt P, Horn L, Spigel D, Soria J-C, Solomon B, Camidge DR, Gadgeel S, Paweletz C, Wu L, Chien S, O'Donnell P, Matheny S, Despain D, Rolfe L, Raponi M, Allen AR, Park K. and Wakelee H, Clin. Cancer Res, 2016, 22, 2386–2395. [PubMed: 26747242]
12. Crowley E, Di Nicolantonio F, Loupakis F. and Bardelli A, Nat. Rev. Clin. Oncol, 2013, 10, 472–484. [PubMed: 23836314]
13. Karachaliou N, Mayo-de las Casas C, Queralt C, de Aguirre I, Melloni B, Cardenal F, Garcia-Gomez R, Massuti B, Sánchez JM, Porta R, Ponce-Aix S, Moran T, Carcereny E, Felip E, Bover I, Insa A, Reguart N, Isla D, Vergnenegre A, de Marinis F, Gervais R, Corre R, Paz-Ares L, Morales-Espinosa D, Viteri S, Drozdowskyj A, Jordana-Ariza N, Ramirez-Serrano JL, Molina-Vila MA and Rosell R, JAMA Oncol., 2015, 1, 149–157. [PubMed: 26181014]
14. Diaz LA Jr and Bardelli A, J. Clin. Oncol, 2014, 32, 579–586. [PubMed: 24449238]
15. Oxnard GR, Thress KS, Alden RS, Lawrance R, Paweletz CP, Cantarini M, Yang JC-H, Barrett JC and Ja PA¨nne, J. Clin. Oncol, 2016, 34, 3375–3382. [PubMed: 27354477]
16. Schwarzenbach H, Hoon DS and Pantel K, Nat. Rev. Cancer, 2011, 11, 426–437. [PubMed: 21562580]
17. FDA, Summary of safety and effectiveness data (SSED), https://www.accessdata.fda.gov/cdrh_docs/pdf15/P150044B.pdf.
18. Castellanos-Rizaldos E, Grimm DG, Tadigotla V, Hurley J, Healy J, Neal PL, Sher M, Venkatesan R, Karlovich C, Raponi M, Krug A, Noerholm M, Tannous J, Tannous BA, Raez LE and Skog JK, Clin. Cancer Res, 2018, 24, 2944–2950. [PubMed: 29535126]
19. Krebs MG, Metcalf RL, Carter L, Brady G, Blackhall FH and Dive C, Nat. Rev. Clin. Oncol, 2014, 11, 129–144. [PubMed: 24445517]
20. Dong J, Chen J-F, Smalley M, Zhao M, Ke Z, Zhu Y. and Tseng H-R, Adv. Mater, 2020, 32, e1903663.

21. Shen Z, Wu A. and Chen X, Chem. Soc. Rev, 2017, 46, 2038–2056. [PubMed: 28393954]
22. Cristofanilli M, Budd GT, Ellis MJ, Stopeck A, Matera J, Miller MC, Reuben JM, Doyle GV, Allard WJ, Terstappen LWMM and Hayes DF, N. Engl. J. Med, 2004, 351, 781–791. [PubMed: 15317891]
23. Shaffer DR, Leversha MA, Danila DC, Lin O, Gonzalez-Espinoza R, Gu B, Anand A, Smith K, Maslak P, Doyle GV, Terstappen LWMM, Lilja H, Heller G, Fleisher M. and Scher HI, Clin. Cancer Res, 2007, 13, 2023–2029. [PubMed: 17404082]
24. Yang L, Lang JC, Balasubramanian P, Jatana KR, Schuller D, Agrawal A, Zborowski M. and Chalmers JJ, Biotechnol. Bioeng, 2009, 102, 521–534. [PubMed: 18726961]
25. He W, Wang H, Hartmann LC, Cheng JX and Low PS, Proc. Natl. Acad. Sci. U. S. A, 2007, 104, 11760–11765. [PubMed: 17601776]
26. Nagrath S, Sequist LV, Maheswaran S, Bell DW, Irimia D, Ulkus L, Smith MR, Kwak EL, Digumarthy S. and Muzikansky A, Nature, 2007, 450, 1235–1239. [PubMed: 18097410]
27. Stott SL, Hsu C-H, Tsukrov DI, Yu M, Miyamoto DT, Waltman BA, Rothenberg SM, Shah AM, Smas ME, Korir GK, Floyd FP, Gilman AJ, Lord JB, Winokur D, Springer S, Irimia D, Nagrath S, Sequist LV, Lee RJ, Isselbacher KJ, Maheswaran S, Haber DA and Toner M, Proc. Natl. Acad. Sci. U. S. A, 2010, 107, 18392–18397. [PubMed: 20930119]
28. Mach AJ, Kim JH, Arshi A, Hur SC and Carlo DD, Lab Chip, 2011, 11, 2827–2834. [PubMed: 21804970]
29. Ozkumur E, Shah AM, Ciciliano JC, Emmink BL, Miyamoto DT, Brachtel E, Yu M, Chen P-I, Morgan B,Trautwein J, Kimura A, Sengupta S, Stott SL, Karabacak NM, Barber TA, Walsh JR, Smith K, Spuhler PS, Sullivan JP, Lee RJ, Ting DT, Luo X, Shaw AT, Bardia A, Sequist LV, Louis DN, Maheswaran S, Kapur R, Haber DA and Toner M, Sci. Transl. Med, 2013, 5, 179ra147.
30. Krivacic RT, Ladanyi A, Curry DN, Hsieh HB, Kuhn P, Bergsrud DE, Kepros JF, Barbera T, Ho MY, Chen LB,Lerner RA and Bruce RH, Proc. Natl. Acad. Sci. U. S. A, 2004, 101, 10501–10504. [PubMed: 15249663]
31. Jack RM, Grafton MMG, Rodrigues D, Giraldez MD, Griffith C, Cieslak R, Zeinali M, Kumar Sinha C, Azizi E, Wicha M, Tewari M, Simeone DM and Nagrath S, Adv. Sci, 2016, 3, 1600063.
32. Ramsköld D, Luo S, Wang Y-C, Li R, Deng Q, Faridani OR, Daniels GA, Khrebtukova I, Loring JF, Laurent LC, Schroth GP and Sandberg R, Nat. Biotechnol, 2012, 30, 777–782. [PubMed: 22820318]
33. Miyamoto DT, Zheng Y, Wittner BS, Lee RJ, Zhu H, Broderick KT, Desai R, Fox DB, Brannigan BW, Trautwein J, Arora KS, Desai N, Dahl DM, Sequist LV, Smith MR, Kapur R, Wu C-L, Shioda T, Ramaswamy S, Ting DT, Toner M, Maheswaran S. and Haber DA, Science, 2015, 349, 1351–1356. [PubMed: 26383955]
34. Kalinich M, Bhan I, Kwan TT, Miyamoto DT, Javaid S, LiCausi JA, Milner JD, Hong X, Goyal L, Sil S, Choz M, Ho U, Kapur R, Muzikansky A, Zhang H, Weitz DA, Sequist LV, Ryan DP, Chung RT, Zhu AX, Isselbacher KJ, Ting DT, Toner M, Maheswaran S. and Haber DA, Proc. Natl. Acad. Sci. U. S. A, 2017, 114, 1123–1128. [PubMed: 28096363]
35. Miyamoto DT, Lee RJ, Kalinich M, LiCausi JA, Zheng Y, Chen T, Milner JD, Emmons E, Ho U, Broderick K, Silva E, Javaid S, Kwan TT, Hong X, Dahl DM, McGovern FJ, Efstathiou JA, Smith MR, Sequist LV, Kapur R, Wu C-L, Stott SL, Ting DT, Giobbie-Hurder A, Toner M, Maheswaran S. and Haber DA, Cancer Discovery, 2018, 8, 288–303. [PubMed: 29301747]
36. Hong X, Sullivan RJ, Kalinich M, Kwan TT, Giobbie-Hurder A, Pan S, LiCausi JA, Milner JD, Nieman LT, Wittner BS, Ho U, Chen T, Kapur R, Lawrence DP, Flaherty KT, Sequist LV, Ramaswamy S, Miyamoto DT, Lawrence M, Toner M, Isselbacher KJ, Maheswaran S. and Haber DA, Proc. Natl. Acad. Sci. U. S. A, 2018, 115, 2467–2472. [PubMed: 29453278]
37. Shen M-Y, Chen J-F, Luo C-H, Lee S, Li C-H, Yang Y-L, Tsai Y-H, Ho B-C, Bao L-R, Lee T-J, Jan YJ, Zhu Y-Z, Cheng S, Feng FY, Chen P, Hou S, Agopian V, Hsiao Y-S, Tseng H-R, Posadas EM and Yu H-H, Adv. Healthcare Mater, 2018, 7, 1700701.
38. Ke Z, Lin M, Chen J-F, Choi J-S, Zhang Y, Fong A, Liang A-J, Chen S-F, Li Q, Fang W, Zhang P, Garcia MA, Lee T, Song M, Lin H-A, Zhao H, Luo S-C, Hou S, Yu H-H and Tseng H-R, ACS Nano, 2015, 9, 62–70. [PubMed: 25495128]
39. Caspersson TO, Symp. Soc. Exp. Biol, 1947, 1, 127–151.

40. Lin M, Chen J-F, Lu Y-T, Zhang Y, Song J, Hou S, Ke Z. and Tseng H-R, Acc. Chem. Res, 2014, 47, 2941–2950. [PubMed: 25111636]

41. Chen J-F, Zhu Y, Lu Y-T, Hodara E, Hou S, Agopian VG, Tomlinson JS, Posadas EM and Tseng H-R, Theranostics, 2016, 6, 1425–1439. [PubMed: 27375790]

42. Jan YJ, Chen J-F, Zhu Y, Lu Y-T, Chen SH, Chung H, Smalley M, Huang Y-W, Dong J, Chen L-C, Yu H-H, Tomlinson JS, Hou S, Agopian VG, Posadas EM and Tseng H-R, Adv. Drug Delivery Rev, 2018, 125, 78–93.

43. Wang S, Liu K, Liu J, Yu ZTF, Xu X, Zhao L, Lee T, Lee EK, Reiss J, Lee YK, Chung LWK, Huang J, Rettig M, Seligson D, Duraiswamy KN, Shen CKF and Tseng H-R, Angew. Chem., Int. Ed, 2011, 50, 3084–3088.

44. Court CM, Hou S, Winograd P, Segel NH, Li QW, Zhu Y, Sadeghi S, Finn RS, Ganapathy E, Song M, French SW, Naini BV, Sho S, Kaldas FM, Busuttil RW, Tomlinson JS, Tseng H-R and Agopian VG, Liver Transplant., 2018, 24, 946–960.

45. Crosbie PA, Shah R, Krysiak P, Zhou C, Morris K, Tugwood J, Booton R, Blackhall F. and Dive C, J. Thorac. Oncol, 2016, 11, 1793–1797. [PubMed: 27468936]

46. Chemi F, Rothwell DG, McGranahan N, Gulati S, Abbosh C, Pearce SP, Zhou C, Wilson GA, Jamal-Hanjani M, Birkbak N, Pierce J, Kim CS, Ferdous S, Burt DJ, Slane-Tan D, Gomes F, Moore D, Shah R, Al Bakir M, Hiley C, Veeriah S, Summers Y, Crosbie P, Ward S, Mesquita B, Dynowski M, Biswas D, Tugwood J, Blackhall F, Miller C, Hackshaw A, Brady G, Swanton C. and Dive C, Nat. Med, 2019, 25, 1534–1539. [PubMed: 31591595]

47. Dong J, Jan YJ, Cheng J, Zhang RY, Meng M, Smalley M, Chen P-J, Tang X, Tseng P, Bao L, Huang T-Y, Zhou D, Liu Y, Chai X, Zhang H, Zhou A, Agopian VG, Posadas EM, Shyue J-J, Jonas SJ, Weiss PS, Li M, Zheng G, Yu H-H, Zhao M, Tseng H-R and Zhu Y, Sci. Adv, 2019, 5, eaav9186.

48. Jan YJ, Yoon J, Chen J-F, Teng P-C, Yao N, Cheng S, Lozano A, Chu GCY, Chung H, Lu Y-T, Chen P-J, Wang JJ, Lee Y-T, Kim M, Zhu Y, Knudsen BS, Feng FY, Garraway IP, Gao AC, Chung LWK, Freeman MR, You S, Tseng H-R and Posadas EM, Theranostics, 2019, 9, 2812–2826. [PubMed: 31244925]

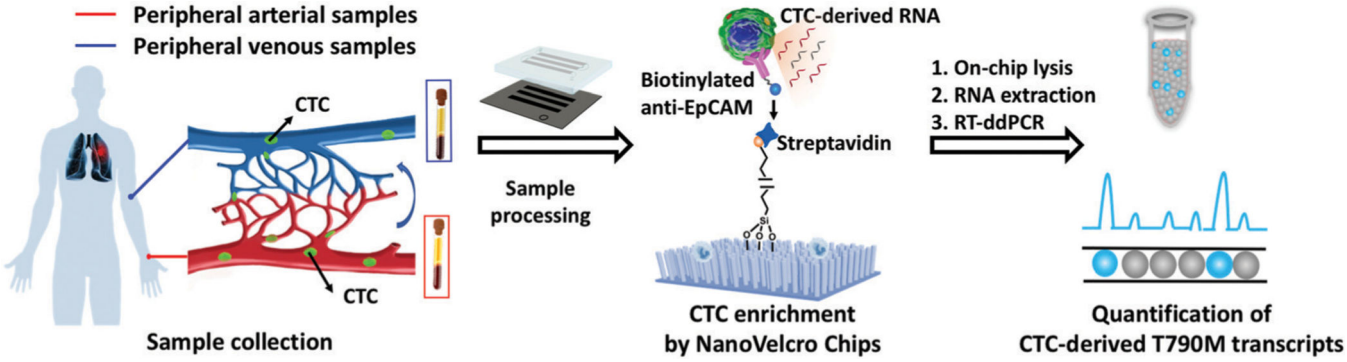

Fig. 1.

Workflow of the NanoVelcro CTC-digital assay for detecting the EGFR T790M mutation. The schematic diagram of the components of the NanoVelcro Chips demonstrates that the polydimethylsiloxane (PDMS)-based chaotic mixer and the channels of the silicon nanowire chip create a microfluidic channel which optimizes cellular interactions with the chip surface. In the cutout, the nanowire substrate can be seen functionalized with streptavidin, used for the enrichment of biotinylated capture antibody (*i.e.*, anti-epithelial cell adhesion molecule, EpCAM) labeled CTCs. Captured CTCs are then lysed in the device to release CTC-derived RNA for downstream analysis *via* RT-ddPCR. We utilize this workflow to quantify T790M transcripts in NSCLC CTCs from peripheral arterial and venous blood samples.

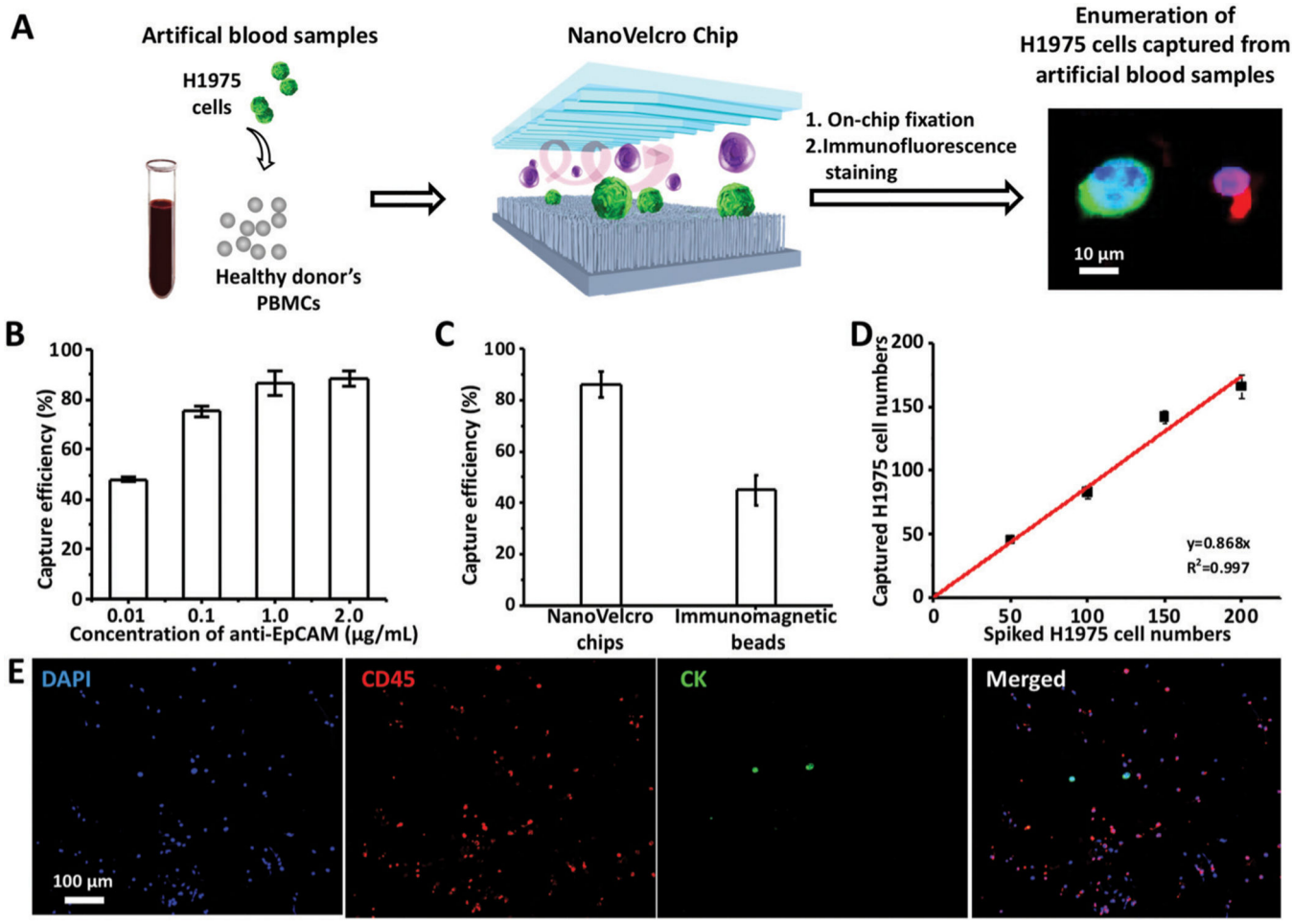

Fig. 2.

Optimization and validation of NanoVelcro Chips for the capture of NSCLC CTCs using artificial blood samples. (A) Workflow summarizes the CTC enrichment of NanoVelcro Chips using artificial blood samples, prepared by spiking H1975 cells in the PBMCs from healthy donors. Immunofluorescence staining was employed to enumerate captured CTCs for calculating the capture efficiency. (B) CTC-capture efficiency of NanoVelcro Chips was studied at anti-EpCAM concentrations of 0.01, 0.1, 1.0 and 2.0 μg mL^{-1}. (C) Comparison of the capture efficiencies of CTCs on NanoVelcro Chips and immunomagnetic beads. (D) Dynamic ranges observed for NSCLC CTC capture efficiency using artificial blood samples spiked with different amounts of H1975 cells under the optimal capture conditions. (E) Representative fluorescence micrographs of WBCs (DAPI+/CK−/CD45+) and CTCs (DAPI +/CK+/CD45−) captured from artificial blood samples using NanoVelcro Chips.

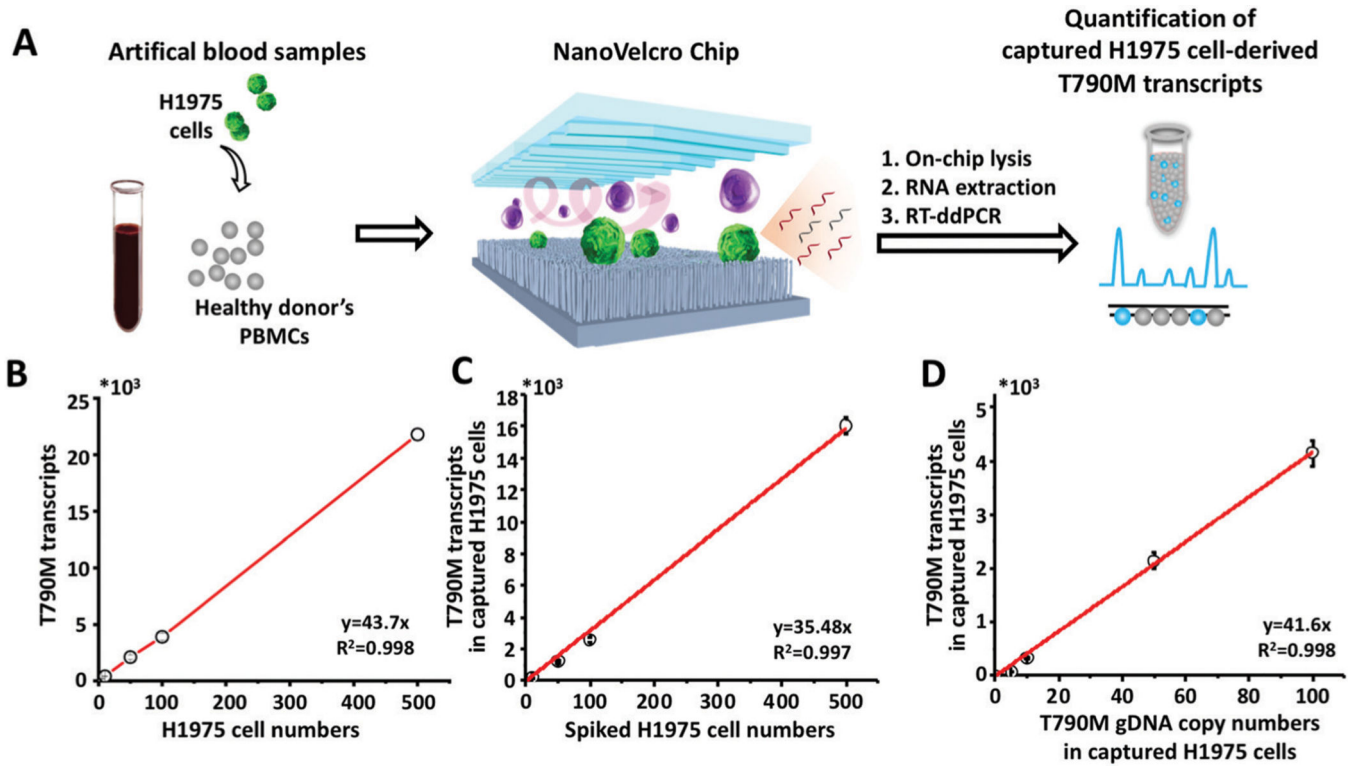

Fig. 3.

Validation of the NanoVelcro CTC-digital assay for quantification of T790M transcripts in NSCLC CTCs using artificial blood samples. (A) A quantitative method was developed for evaluating the performance of the NanoVelcro CTC-digital assay using artificial blood samples, prepared by spiking H1975 cells into the PBMCs from healthy donors. An RT-ddPCR was employed to quantify the T790M transcripts in H1975 cells. (B) ddPCR quantitation of the T790M transcripts in different amounts of H1975 cells. (C) ddPCR quantitation of the T790M transcripts from captured CTCs in artificial blood samples spiked with different amounts of H1975 cells. (D) Linear correlation of the copy numbers of the T790M transcripts and the T790M gDNA copy numbers in different amounts of spiked H1975 cells processed by the NanoVelcro CTC-digital assay.

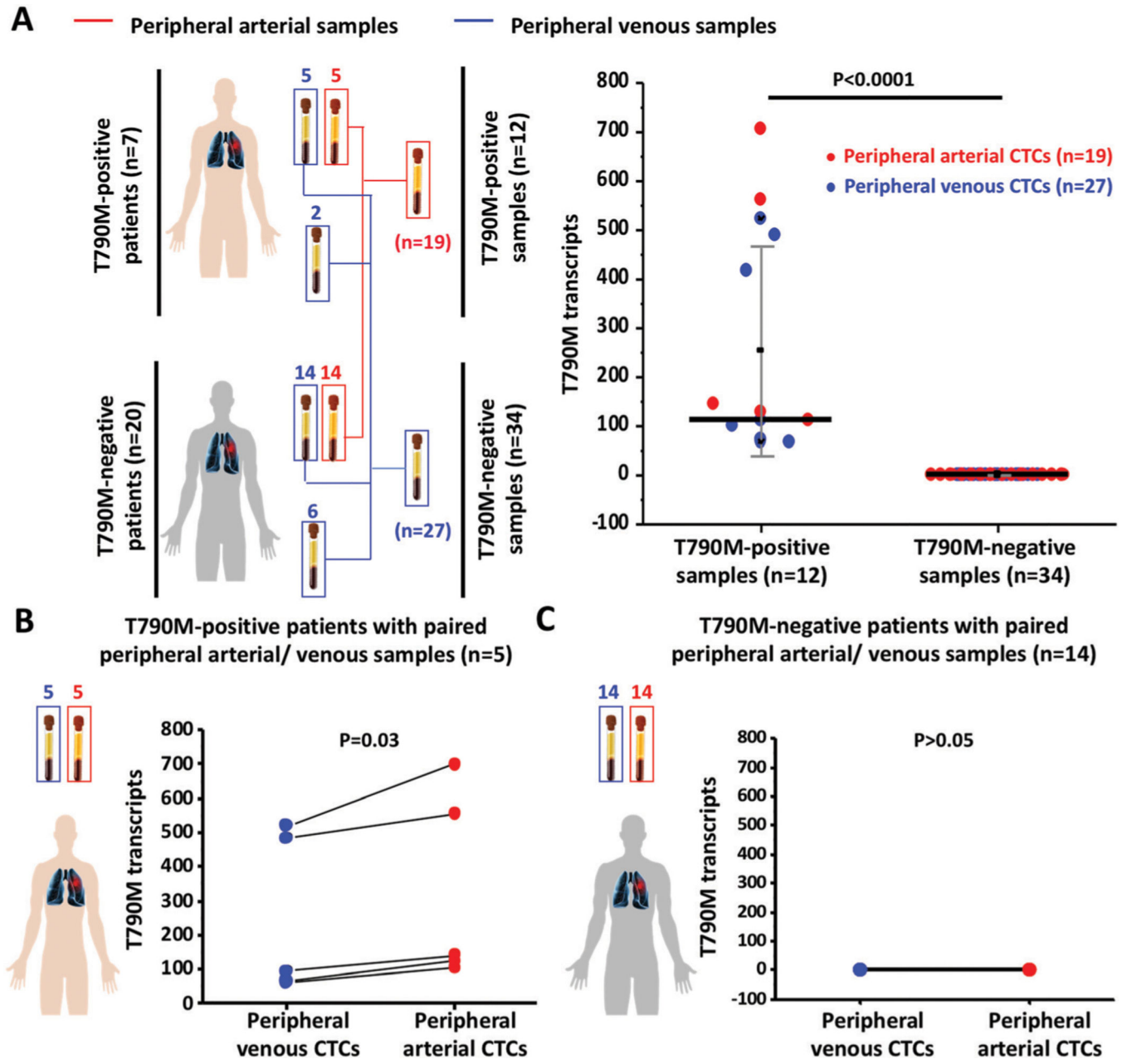

Fig. 4.

Statistical analysis of T790M transcripts in CTCs captured from peripheral arterial/venous blood samples of advanced NSCLC patients. (A) Comparison of the copy numbers of T790M transcripts in CTCs captured from peripheral arterial/venous blood samples between T790M-positive and T790M-negative NSCLC patients. (B) Comparison of the copy numbers of T790M transcripts between peripheral arterial CTCs and matched peripheral venous CTCs in T790M-positive patients. (C) Comparison of the copy numbers of T790M transcripts between peripheral arterial CTCs and matched peripheral venous CTCs in T790M-negative patients.

Table 1

Clinical characteristics of advanced NSCLC patients enrolled in this study

							Copy numbers of T790M transcripts in CTCs[a]	
Patient	**Gender**	**Age (y)**	**Smoking (y)**	**Clinical stage**	**T790M mutation status (tissue/cfDNA)**	**Osimertinib treatment**	**Arterial CTCs[b]**	**Venous CTCs**
P1	F	44	0	IV	+	Yes	126	68
P2	M	60	30	IV	+	Yes	558	486
P3	M	69	0	IV	+	Yes	702	522
P4	M	59	30	IV	+	Yes	N/A	108
PS	M	40	0	IV	+	Yes	N/A	414
P6	F	55	0	IV	+	No	144	97.2
P7	M	59	10	IV	+	Yes	108	64.8
P8	M	58	0	IV	—	No	—	—
P9	F	85	0	IV	—	No	—	—
P10	F	64	0	IV	—	No	—	—
P11	F	56	0	IV	—	No	—	—
P12	F	73	0	IV	—	No	—	—
P13	M	64	40	IV	—	No	—	—
P14	M	68	50	IV	—	No	—	—
P15	F	36	0	IV	—	No	—	—
P16	M	83	0	IV	—	No	—	—
P17	F	54	0	IV	—	No	—	—
P18	F	74	0	IV	—	No	—	—
P19	F	82	0	IV	—	No	—	—
P20	F	75	0	IV	—	No	N/A	—
P21	M	47	0	IV	—	No	N/A	—
P22	F	65	0	IV	—	No	N/A	—
P23	M	52	20	IV	—	No	N/A	—
P24	M	69	0	IV	—	No	N/A	—
P25	F	74	0	IIIC	—	Yes	—	—
P26	F	63	0	IV	—	Yes	—	—
P27	F	50	0	IV	—	Yes	N/A	—

[a] Per 2 mL blood.

[b] N/A: arterial samples not available.